DOI 10.1007/s10812-017-0434-2
Journal of Applied Spectroscopy, Vol. 84, No.1, March, 2017 (Russian Original Vol. 84, No. 1, January–February, 2017)

ANALYSIS OF MANGANESE IN SOIL USING LASER-INDUCED BREAKDOWN SPECTROSCOPY

J. Yongcheng,[a,b] H. Jiang,[b] J. Benchi,[b] and L. Dong[c*] UDC 621.373.8;543.42:546.711

Laser-induced breakdown spectroscopy (LIBS) has been applied to measure spectral characteristics and to perform quantitative analysis of the concentration of manganese in soil, an issue of great concern for precision agriculture. For the analysis, soil samples were compressed into pellets and a pulsed Nd:YAG laser was employed to produce the plasma in air at atmospheric pressure. Using this approach, we analyzed the time evolution of spectral characteristics and their dependence on the laser pulse energy. A calibration curve was constructed using reference sandy soil samples collected from a farm. An internal standard curve was used to improve the accuracy of the LIBS metrology for soil analyses. The results of this analysis demonstrated the usefulness of this method for analyzing the concentration of manganese in soil.

Keywords: *laser-induced breakdown spectroscopy, soil, manganese.*

Introduction. Laser-induced breakdown spectroscopy (LIBS) technique is a type of atomic emission spectroscopy, based on the spectral analysis of characteristic emission using micro-plasma for the determination of the elemental composition of a sample [1]. Traditional analytical methods such as inductively coupled plasma (ICP) and atomic absorption spectrometry (AAS) routinely require a sample-preparation procedure and the use of standards for each determined element. Compared with these methods, LIBS exhibits several advantages, including high sensitivity, real-time response, multi-element measurements, and minimum sample preparation. However, spectrochemical analysis by LIBS is determined not only by the concentration of the analyte in the sample, but also by the experimental conditions, e.g., delay time, laser characteristics, sample characteristics, atmosphere gas, and other parameters [2]. Thus, a detailed analysis of such experimental parameters is required to obtain a reliable quantitative result. The most common approach to perform the quantitative LIBS analysis is the calibration curve method with matrix-matched standards. When using a matrix element in a sample as an internal standard element to construct the internal standard curve [3], the accuracy of the LIBS metrology can be improved.

The LIBS technique has been used in various fields [4–8]. Of particular interest is the application of LIBS in agriculture for studying heavy metal pollution [9], soil fertility [10], plant materials [11], and fertilizers [12]. Precision agriculture is a farming management concept based on observing, measuring, and responding to inter- and intra-field variability in crops and soils. Precision fertilization is a key component of precision agriculture. It involves dividing the field into grids using a geographical positioning system, testing for soil nutrients, and computing the fertilizer input needed with a fertilization model. Finally, the fertilization is performed using a variable rate applicator. The determination of nutrient elements in soil has therefore been studied in the literature because of its importance for precision fertilization [13–16]. The aforementioned research has focused on total C, inorganic C, organic C, total N, and total P in soil. Few investigations have been devoted to analyzing the manganese (Mn) in soil [17–19]; these studies carried out qualitative analysis, and only a few works have involved quantitative analysis [19]. This may be attributed, in part, to the limited amount of attention that has been paid to the role of Mn in plant metabolism and growth. However, Mn in soil has a clear function in the photosynthesis and metabolism of plants and can promote growth, disease resistance, and increased output [20]. The oxide and hydrates of Mn have good surface activation and degrading functions for organic pollution in soil. Hence, it is important to optimize the experimental parameters together with the investigation of new strategies of calibration for the LIBS analysis of Mn in soil [21].

*To whom correspondence should be addressed.

[a]School of Electric Engineering and Automation, Anhui University, Hefei 230601, China; [b]School of Mechanical and Automotive Engineering, Hefei University of Technology, Hefei 230009, China; [c]School of Electronics & Information Engineering, Anhui University, Hefei 230601, China; e-mail: dliang@ahu.edu.cn. Published in Zhurnal Prikladnoi Spektroskopii, Vol. 84, No. 1, pp. 120–126, January–February, 2017. Original article submitted March 18, 2016.

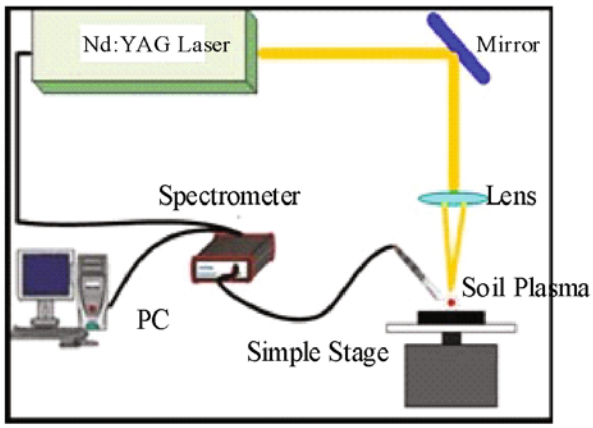

Fig. 1. Schematic of the LIBS experimental system.

In the present work, we applied the LIBS technique to determine the concentration of Mn in soil with the goal of precision fertilization. A sandy soil sampled from a farmland area was used as the testing sample. We observed the emission line of Mn, and the temporal evolution of the spectral emission was analyzed. We analyzed the effect of the laser pulse energy on the spectral features and provided a quantitative analysis of Mn.

Experimental. We collected 33 soil samples from a rice field located at Huaiyuan, Bengbu, China (latitude coordinate: 32°95', longitude coordinate: 117°19'). The sampling position was 10–25 cm below the ground, which was considered the main area in which plant roots absorb micronutrients. The collected soil was dried, ground to grain size, and sieved using a mesh size of 1 mm. For each sample, we used 5 g of the soil sample to prepare pellet. After this, the soil was pressed in a mold to form a pellet of approximately 3-cm diameter and 2-cm thickness. The reference concentrations of Mn in these soil samples were analyzed by inductively coupled plasma-mass spectrometry (ICP-MS), the range of concentration was 250–1500 mg/kg.

The experimental setup employed is shown in Fig. 1. A Q-switched Nd:YAG laser (Ultra ICE 450, 1064 nm, 6 ns pulse FWHM, 200 mJ/pulse, repetition rate of 1 Hz) was used to generate the plasmas on the pellet. The laser beam was focused with a 2.5-cm diameter, 10-cm focal length convex lens to create the plasma. The light emitted from the plasma was collected by a fused silica quartz lens of 4 cm focal length and focused into the entrance slit of a multiple spectrometer. The spectrometer (Avantes-2048-USB2, Netherlands) has three channels containing separate gratings and charge-coupled device arrays, and all spectra are taken simultaneously in the wavelength range of 190–510 nm. Finally, the spectra were recorded and processed using a personal computer. A homemade gate pulse generator was employed to trigger the laser and the spectrometer. When triggered, it produced a burst of pulses that were used to fire the laser and trigger the spectrometer after a set delay time.

During the experiment, the sample pellet was mounted on an *x–y* rotary stage, which was constantly rotated with a stepper motor to minimize soil heterogeneity. Twenty laser pulses were used to clean the sample surface before the measurements were taken. For each soil sample, the measurement was repeated 10 times, and 20 spectra were averaged for each measurement to improve the signal/noise ratio and reduce statistical error as the energy of the laser pulse fluctuated from pulse to pulse. The experimental data were plotted and analyzed using an ORIGIN 8.0 software.

Results and Discussion. *LIBS spectra of a soil sample.* Each component of a LIBS detection system has a certain spectral response that depends on wavelength. We performed an intensity calibration of the spectral response using deuterium and tungsten halogen lamps (DH-2000-DUV, Ocean Optics, USA). Figure 2 shows the LIBS spectra of the soil pellets. It represents 20 averaged spectra of a soil pellet in the range of 400–410 nm, which include the emission lines of Mn and Fe in soil.

The soil composition is very complex, and spectral overlap is common. Thus, when the LIBS technique is used to analyze the soil sample, the resolution of the spectrometer is an important parameter. The lines of Mn at 403.1, 403.3, and 403.4 nm are clearly visible in the spectrum. The emission line of 403.1 nm was selected as the analytical line for Mn. Because this line was not subject to interference by other elements, the line intensity was relatively large.

The principles for selecting a matrix element in a sample as the internal standard element are as follows: (1) the concentration must be approximately constant and the concentration range should not be too low or too high; (2) the physical

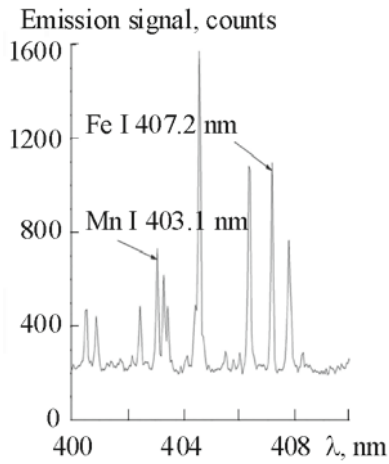

Fig. 2. Averaged LIBS spectrum of soil sample in the range of 400–410 nm (n = 20).

TABLE 1. Reference Concentration (g/kg) of Fe in 33 Soil Samples

Sample	[Fe]	Sample	[Fe]	Sample	[Fe]	Sample	[Fe]	Sample	[Fe]	Sample	[Fe]
1	0.3489	7	0.3491	13	0.3514	18	0.3485	24	0.3507	29	0.3516
2	0.3483	8	0.3484	14	0.3510	19	0.3487	25	0.3519	30	0.3506
3	0.3486	10	0.3512	15	0.3509	20	0.3492	26	0.3509	31	0.3518
4	0.3488	11	0.3507	16	0.3492	21	0.3487	27	0.3517	32	0.3511
5	0.3493	12	0.3513	17	0.348	22	0.3494	28	0.3515	33	0.3505
6	0.3489										

and chemical properties of the internal standard element and analytical element should be similar; (3) the wavelength of the analytical element and the internal standard element should be close, and the self-absorption phenomenon should not occur for the internal standard element; and (4) when selecting the atomic spectra as the line spectrum pair, the excitation potential of the analytical element and the internal standard element should be sufficiently similar. Based on these principles, we selected Fe as the matrix element of soil. The concentrations of Fe were approximately identical in all soil samples, as shown in Table 1. The spectrum of Fe at 400–410 nm contained lines at 404.6, 406.4, and 407.2 nm. Thus, based on the principles of selecting the internal standard element, the emission line of Fe 407.2 nm was selected as the internal standard line.

Time evolution characteristics of the manganese element in soil. The measurements were performed with temporal resolution using a suitable delay time in the range of 1.28–5.08 μs with a gate width of 1.05 ms (which is the minimum value of the spectrometer). Figure 3a shows the relationship between the delay time and the intensity of the characteristic line of Mn. We observed that the peak value of the characteristic line increased quickly at first, then decreased with the delay time. The maximum value occurred at 1.68 μs. The signal-to-background ratio (SBR) of the characteristic line as a function of delay time is presented in Fig. 3b. The analysis provides an optimized delay time of 1.88 μs by maximizing the SBR. The main reasons for this observation are as follows: at the initial plasma stage, the continuous spectrum is very strong. However, with increasing delaytime, the continuous spectrum weakens and the characteristic line of Mn strengthens, thus increasing the SBR. Then, with further increase in the delay time, the plasma light weakens and SBR is reduced. Therefore, the optimal delay time in the experiment was set at 1.88 μs.

Spectral characteristics of manganese element by the influence of laser pulse energy. The changes of laser pulse energy can be realized by regulating the attenuator of the optical path. The line intensity of Mn was measured from plasma generated under the delay time of 1.88 μs with the laser pulse energy varying from 40 to 165 mJ/pulse. These results are shown in Fig. 4a. The intensity of the characteristic line of Mn increased when the laser pulse energy was increased. Sufficient

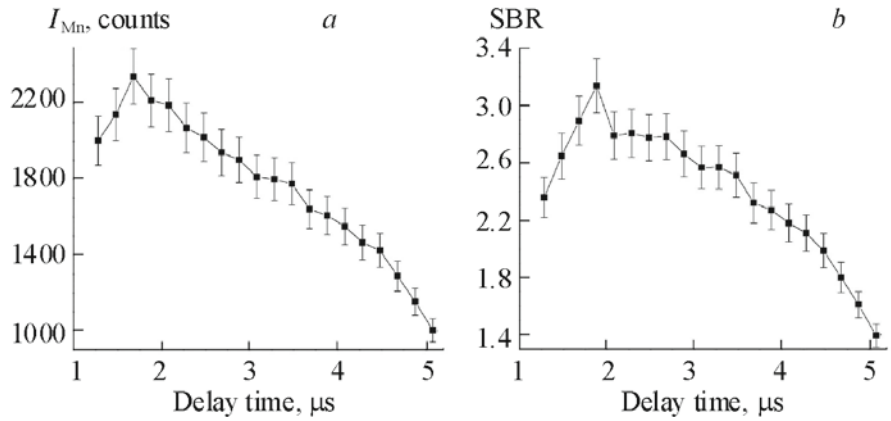

Fig. 3. Relationship between delay time and the characteristic line of Mn at 403.1 nm: (a) the intensity and (b) SBR changes with delay time.

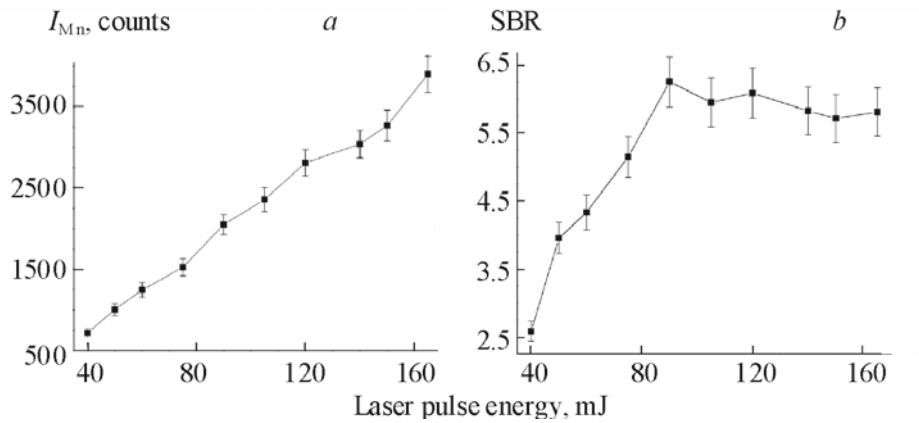

Fig. 4. Line intensity of Mn at 403.1 nm (a) and SBR of spectrum (b) depending on laser pulse energy.

energy can not only reduce the noise caused by the instability of the laser generator, but also enhance the intensity of the line. The absorption of the laser pulse energy by the high-density plasma is the main reason for this phenomenon [22].

Figure 4b illustrates the SBR as a function of the laser pulse energy. When the laser pulse energy increased from 40 to 90 mJ/pulse, the SBR increased. The SBR was approximately 6, while the laser pulse energy varied from 90 to 165 mJ/pulse. When the laser pulse energy increased, the plasma temperature correspondingly increased [23]. Simultaneously, the sufficient energy reduced the background radiation intensity and the amount of noise caused by the instability of the laser generator. Thus, the SBR increased with increase in laser pulse energy; however, when the laser pulse energy was above 90 mJ, the SBR was approximately constant. Therefore, the laser pulse energy used for constructing the calibration curve of Mn was set at 90 mJ.

Quantitative analysis using the calibration curve and internal standard method. We used 23 of all 33 soil samples, with Mn concentrations in the range of 250–1500 mg/kg, to construct the calibration model. The calibration curve was constructed using the line intensity (peak intensity minus background) of Mn at 403.1 nm versus the corresponding concentration, as shown in Fig. 5a. Figure 5a indicates the linear trend between line intensity and concentration with a coefficient of correlation of 0.825. The limit of detection ($C_L = 3\sigma_s/m$) was 86.7 mg/kg for Mn in soil, which is better than the results reported by Popov et al. [19]. Ten soil samples, as unknown samples, were used to estimate the ability and prediction accuracy of the LIBS technique for analyzing the Mn concentration. All 33 soil samples were measured under the same experimental conditions. According to the obtained calibration curve, we first calculated the Mn concentration of the unknown samples. The relation between the LIBS predicted concentration and the reference concentration for Mn is shown in Fig. 5b, with a correlation coefficient of 0.934. The absolute error was defined as the absolute value of the difference between the measured

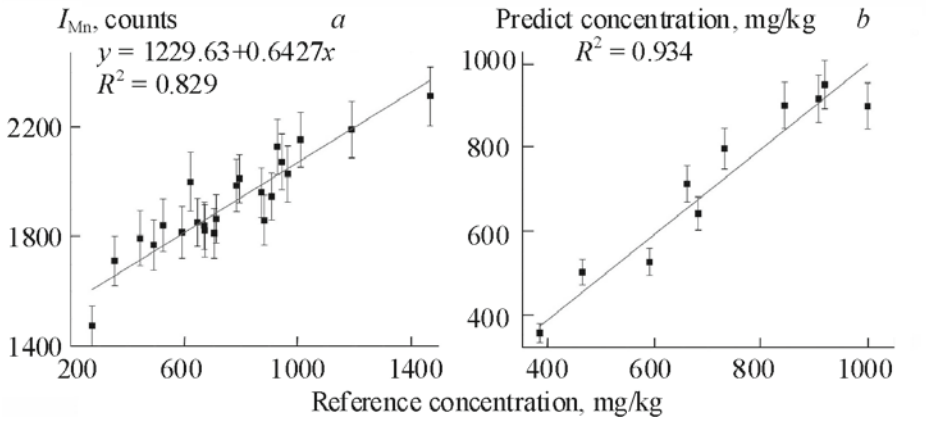

Fig. 5. Calibration curve for the spectral line of Mn at 403.1 nm (a) and comparison of Mn concentration predicted by LIBS and the reference value (ICP-MS) (b).

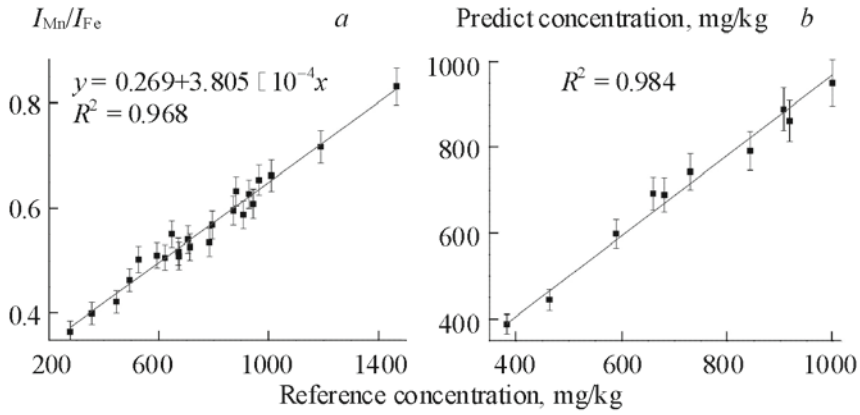

Fig. 6. Internal standard method: (a) calibration curve using Fe as an internal standard element and (b) comparison of Mn concentration predicted by LIBS and the reference value (ICP-MS).

concentration and the reference concentration (ICP-MS), while the relative error was defined as the absolute error divided by the reference concentration. The absolute errors of Mn are in the range of 11.3–98.1 mg/kg, with the relative errors in the range of 2.25–10.7%. Both the correlation coefficient and the relative error should be improved for further quantitative analysis.

As a nondestructive measurement and analysis technique, the result of the spectrochemical analysis by LIBS depends on the experimental conditions discussed above. Through selecting the internal standard element [24] and calculating the line intensity ratio of the analytical element and the internal standard element, the internal standard curve can be constructed. The ratio of Mn line intensity (403.1 nm) to that of Fe (407.2 nm) versus the concentration of Mn in soil was used for calibration. The internal standard curve that was obtained is shown in Fig. 6a. The coefficient of correlation of the straight line fit was 0.969.

Similar to the method used in the calibration curve, Fig. 6b shows the relation between the LIBS predicted concentration and the reference concentration for Mn. The correlation coefficient was increased to 0.984 and the slope was 0.94. The absolute errors between the reference and LIBS measurement concentrations of Mn are in the range of 5.7–55.8 mg/kg, while the relative errors are 1.31–6.09%. The average absolute and relative errors of Mn are 26.2 mg/kg and 3.42%, respectively. Thus, the measurement accuracy of this result can meet the measurement requirements [25]. This also demonstrates that the internal standard method can partly eliminate the instability of the LIBS signal. Validation with the unknown samples indicates that LIBS can be used to measure Mn in soil.

Conclusions. The LIBS technique was applied for quantitative analysis of Mn in soil. To optimize the experimental conditions, the 403.1 nm line was selected as the analytical line for Mn. The optimal delay time was identified as 1.88 μs, based on the time evolution characteristics of the analytical line. The effect of the laser pulse energy on the LIBS spectrum

characteristics was examined to obtain high SBR, and the laser pulse energy was set at 90 mJ. We also made a quantitative analysis based on the calibration curve and internal standard method. The 403.1 and 407.2 nm lines were selected as the analytical line and the internal line of Mn, respectively. The limit of detection of manganese was 86.7 mg/kg. The internal standard method was found to be better than the calibration method because the correlation coefficient of the measurement results of LIBS to ICP-MS for the former was 0.984, while that of the latter was 0.934. Moreover, the average relative error for the internal standard method was only 3.42%. Thus, the internal standard method can improve the accuracy and precision of the measurements. The results in this study therefore provide the basis for the real-time analysis of Mn in soil.

Acknowledgments. The authors gratefully acknowledge the Anhui University of Traditional Chinese Medicine (Hefei, China) for the analysis of elemental concentration in soil. This work has been supported by the National Natural Science Foundation of China (No. 61505001).

REFERENCES

1. A. W. Miziolek, V. Palleschi, and I. Schechter, *Laser-Induced Breakdown Spectroscopy (LIBS): Fundamentals and Applications*, Cambridge University Press, New York (2006).
2. D. W. Hahn and N. Omenetto, *Appl. Spectrosc.*, **64**, No. 12, 335A–366A (2010).
3. D. A. Cremers and L. J. Radziemski, *Handbook of Laser-Induced Breakdown Spectroscopy*, Cambridge University Press, New York, 110–111 (2006).
4. D. Alamelu, A. Sarkar, S. K. Aggarwal, *Talanta*, **77**, No. 1, 256–261 (2008).
5. M. Corsi, G. Cristoforetti, M. Hidalgo, S. Legnaioli, V. Palleschi, A. Salvetti, E. Tognoni, and C. Vallebona, *Appl. Opt*., **42**, No. 30, 6133–6137 (2003).
6. F. J. Wallis, B. L. Chadwick, and R. J. S. Morrison, *Appl. Spectrosc*., **54**, No. 8,1231–1235 (2000).
7. A. C. Samuels, F. C. Delucia Jr., K. L. McNesby, and A. W. Miziolek, *Appl. Opt*., **42**, No. 30, 6205–6209 (2003).
8. Z. A. Arp, D. A. Cremers, R. C. Wiens, D. M. Wayne, B. Salle, and S. Maurice, *Appl. Spectrosc*., **58**, No. 8, 897–909 (2004).
9. Gao Xun, Du Chuang, Shao Yan, Song Xiao-Wei, Zhao Zhen-Ming, Hao Zuo-Qiang, and Lin Jing-Quan, *Acta Phys. Sin.*, **63**, No. 9, 045202 (2014).
10. D. Diaz, D. W. Hahn, and A. Molina, *Appl. Spectrosc*., **66**, No. 1, 99–106 (2012).
11. M. da Silva Gomes, D. Santos Jr., L. Cristina Nunes, G. Gustinelli Arantes de Carvalhob, F. de Oliveira Leme, and F. José Krug, *Talanta*, **85**, 1744–1750 (2011).
12. Shunchun Yao, Jidong Lu, Junyan Li, Kai Chen, Jun Li, and Meirong Dong, *J. Anal. At. Spectrom*., **25**, 1733–1738 (2010).
13. Krishna K. Ayyalasomayajula, Fang Yu-Yueh, Jagdish P. Singh, Dustin L. McIntyre, and Jinesh Jain, *Appl. Opt*., **51**, B149–B154 (2012).
14. R. S. Bricklemyer, D. J. Brown, J. E. Barefield, and S. M. Clegg, *Soil Sci. Soc. Am. J*., **75**, No. 3, 1006–1018 (2001).
15. D. M. Dong, C. J. Zhao, W. G. Zheng, X. D. Zhao, and L. Z. Jiao, *Spectrosc. Lett*., **46**, 421–426 (2013).
16. Cuiping Lu, Liusan Wang, Haiying Hu, Zhong Zhuang, Yubing Wang, Rujing Wang, and Liangtu Song, *Chin. Opt. Lett*., **11**, 053004 (2013).
17. F. Capitelli, F. Colao, M. R. Provenzano, R. Fantoni, G. Brunetti, and N. Senesi, *Geoderma*, **106**, Nos. 1–2, 45–62 (2002).
18. G. S. Senesi, M. Dell'Aglio, R. Gaudiuso, A. DeGiacomo, C. Zaccone, O. DePascale, T. M. Miano, and M. Capitelli, *Environ. Res*., **109**, No. 4, 413–420 (2009).
19. A. M. Popov, F. Colao, and R. Fanton, *J. Anal. At. Spectrom*., **25**, 837–848 (2010).
20. Tian Qiuying, Liu Nana, Bai Wenming, Li Linghao, Chen Jiquan, Reich Peter B., Yu Qiang, Guo Dali, Smith Melinda D., Knapp Alan K., Cheng Weixin, Lu Peng, Gao Yan, Yang An, Wang Tianzuo, Li Xin, Wang Zhengwen, Ma Yibing, Han Xingguo, and Zhang Wen-Hao, *Ecology*, **97**, 65–74 (2016).
21. I. Bassiotis, A. Diamantopolou, A. Giannoudakos, F. Roubani-Kalantzopoulou, and M. Kompitsas, *Spectrochim. Acta*, *B*, **56**, No. 6, 671–683 (2001).
22. Zhang Yu-zhu, Wang Guang-an, Shen Zhong-hua, Ni Xiao-wu, and Lu Jian, *High Power Laser Particle Beams*, **19**, No. 4, 585–588 (2007).
23. A. H. Galmed and M. A. Harith, *Appl. Phys. B*, **91**, Nos. 3–4, 651–660 (2008).
24. Cui Zhifeng, Zhang Xianyi, Yao Guanxin, Wang Xiaoli, Xu Xinsheng, Zheng Xianfeng, Feng Eryin, and Ji Xuehan, *Acta Phys. Sin.*, **55**, No. 9, 4506–4513 (2006).
25. J. B. Sirven, B. Bousquet, L. Canioni, and L. Sarger, *Anal. Chem*., **78**, No. 5,1462–1469 (2006).